Research Article | Vol. 31, No. 8 / 10 Apr 2023 / Optics Express 13317
Optics EXPRESS

Optical rectification and electro-optic sampling in quartz

VASILEIOS BALOS,[1,2] MARTIN WOLF,[1] SERGEY KOVALEV,[3] AND MOHSEN SAJADI[1,4,*]

[1]Fritz Haber Institute of the Max Planck Society, Berlin, Germany
[2]IMDEA Nanociencia, Ciudad Universitaria de Cantoblanco, Madrid, Spain
[3]Helmholtz Zentrum Dresden Rossendorf, Dresden, Germany
[4]Department of Chemistry, University of Paderborn, Paderborn, Germany
*sajadi@fhi-berlin.mpg.de

Abstract: We report the electro-optic sampling (EOS) response and the terahertz (THz) optical rectification (OR) of the z-cut α-quartz. Due to its small effective second-order nonlinearity, large transparency window and hardness, freestanding thin quartz plates can faithfully measure the waveform of intense THz pulses with MV/cm electric-field strength. We show that both its OR and EOS responses are broad with extension up to ~8 THz. Strikingly, the latter responses are independent of the crystal thickness, a plausible indication of dominant surface contribution to the total second-order nonlinear susceptibility of quartz at THz frequencies. Our study introduces the crystalline quartz as a reliable THz electro-optic medium for high field THz detection, and characterize its emission as a common substrate.

Electromagnetic radiation with energies in meV range, known as terahertz (THz) radiation is highly relevant for basic science and for diverse technological applications [1–5]. Weak THz waves are typically used for probing and interrogating the low-energy resonances of matter, including rotations and vibrations of molecules [6–10], intraband transitions [11] and charge transport mechanisms [12–14] in semiconductors, energy gaps in superconductors [15,16], collective intermolecular dynamics of liquids [17,18] and biological systems such as DNA [19], proteins [20] and other bio-relevant systems [21–24].

There is also a growing interest to use intense THz pulses for nonlinear spectroscopy [25–28] and for the control of physical properties of matter [12,29–32]. Thanks to the advances in THz technology, short THz pulses with a few MV/cm electric field strength and more than 1 Tesla magnetic-field are routinely available from table-top sources [31,33]. Although, the race in this field on introducing the novel media with high efficiency in converting the optical pump power into THz radiation [34–37], an opposite route has to be taken for coherent detection and characterization of intense THz pulses.

To measure the waveform of THz pulses one typically employs electro-optic sampling (EOS) [38–40], an approach based on the Pockels effect for characterizing the waveform of THz pulses with high temporal resolution. However, strong THz fields easily saturate EOS signals in conventional electro-optic media. To avoid this, one needs to reduce the THz field power by introducing additional optics e.g., polarizers or multiple silicon plates [41]. Alternatively, one can use electro-optic media whose nonlinearities are small enough to sustain THz electric fields in MV/cm regime without saturating the measured signals.

In this quest, we study the EOS response as well as the optical rectification (OR) signal of z-cut α-quartz (hereafter simply called quartz). The trigonal lattice structure of quartz lacks centrosymmetry [42,43], thereby one may resolve its EOS and OR responses [44]. Notably, the quartz's second order nonlinearity depicted in its effective second-order susceptibility $d_{eff} \approx 1$ pm/V is about two orders of magnitude smaller than that of ZnTe ($d_{eff} = 68.5$ pm/V) [45], a

#480339 https://doi.org/10.1364/OE.480339
Journal © 2023 Received 15 Nov 2022; revised 20 Feb 2023; accepted 23 Feb 2023; published 7 Apr 2023

Optics EXPRESS

commonly used nonlinear medium for THz generation and its coherent detection [46]. Quartz also has a large indirect electronic band gap, 5.7 eV, accompanied by a large transparency window, ranging from λ≈3.5 μm to λ≈200 nm and also it is transparent at the THz frequency range [47]. In addition, quartz is a hard crystalline material with high optical damage threshold, which makes it an excellent candidate for preparing freestanding ultra-thin EOS media.

In this contribution we introduce ultra-thin quartz plates as excellent EO media for resolving the waveform of intense THz electric fields, faithfully. Moreover, as quartz is often used as the substrate in THz emission experiments [48,49], we have characterized its THz emission.

The details of our experimental setup is given elsewhere [27,33]. Briefly, as schematically shown in Fig. 1, quartz plates with different thicknesses are used both as the THz emitter and also electro-optic medium. In Fig. 1(a) quartz plates with different thicknesses are used as EO media. The intense THz pulses are generated either via optical rectification in a Lithium Niobate ($LiNbO_3$, LN) crystal, using the pulse tilting approach [41,50], or using a large-scale spintronic THz emitter (STE) [34,51]. The LN THz pulse peaks at ~1THz, with bandwidth of about ~1.5 THz and more than 2 MV/cm electric-field strength. The STE emission on the other hand is very broad, with a bandwidth exceeding 10 THz and electric-field strength of about 300 kV/cm.

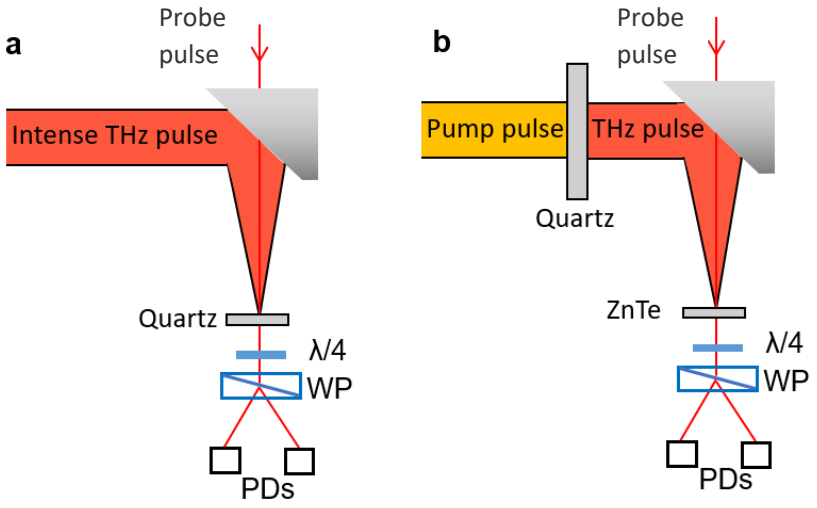

Fig. 1. Schematic of THz generation and detection setups. a) Quartz plates with different thicknesses are used as the nonlinear media for electro-optic sampling (EOS) of intense THz pulses. b) THz emission from the quartz plates is measured in EOS configuration, where the nonlinear medium is a thin ZnTe crystal. λ/4: quarter wave-plate, WP: Wollaston prism, PDs: two photodiodes for balance detection.

Figure 1(b) depicts the THz emission setup in which quartz plates are used as the active medium. Here, 800 nm short laser pulses (Energy: 4 mJ, duration: 30 fs, 10 mm diameter) are used to pump the quartz plates in a collinear geometry. In this scheme a ZnTe crystal (500 μm thick) or GaP crystal (250 μm thick) are used for the EOS of the emitted THz pulses from the quartz plates.

For EOS, temporally delayed probe pulses (Energy: 2 nJ, Wavelength: 800 nm, duration: 8 fs), derived from a seed laser oscillator (Venteon One), are mixed with THz pulses on electro-optic media. The probe pulses are linearly polarized, parallel to the pump polarization, before the sample and subsequently acquire ellipticity owing to the birefringence induced by the co-propagating THz pulse. The ellipticity is detected with a combination of a quarter-wave plate and a Wollaston prism which splits the incoming beam in two perpendicularly polarized beams with power P_1 and P_2. The normalized difference $(P_1 - P_2)/(P_1 + P_2)$ is twice the probe

Optics EXPRESS

ellipticity and measured by two photodiodes as a function of temporal delay between THz pump and optical probe pulse. The quartz plates with thicknesses 5 mm, 1 mm, 0.5 mm, 100 μm, 50 μm are all z-cut and acquired commercially. The thinnest 3 μm thick plate is prepared by polishing the 50 μm thick quartz plate.

1. THz emission

Here we consider the THz emission from quartz crystals with different thicknesses. Figure 2 encompasses the major results. The top panel of Fig. 2(a) shows the emission from 5 mm thick quartz. Two well separated THz emissions, delayed by ~9.3 ps are resolved. The middle panel shows the THz emission from 1 mm thick quartz, again with two separated pulses with 1.8 ps time delay. Note also that the latter signal is measured with 500 μm thick ZnTe crystal, by which only the low frequency part of THz pulse is resolved, hence its waveform is broader than the other crystals. For the thinnest quartz plate, 3 μm thick, only one THz pulse can be discerned. The Fourier spectra of the THz pulses from 5 mm thick quartz (pulse 1) and the emission from 3 μm thick quartz are given in Fig. 2(b). Notably the two spectra display the same profile, where the sharp peak at ~4 THz refers to the low-frequency IR-active phonon mode of quartz [47]. The

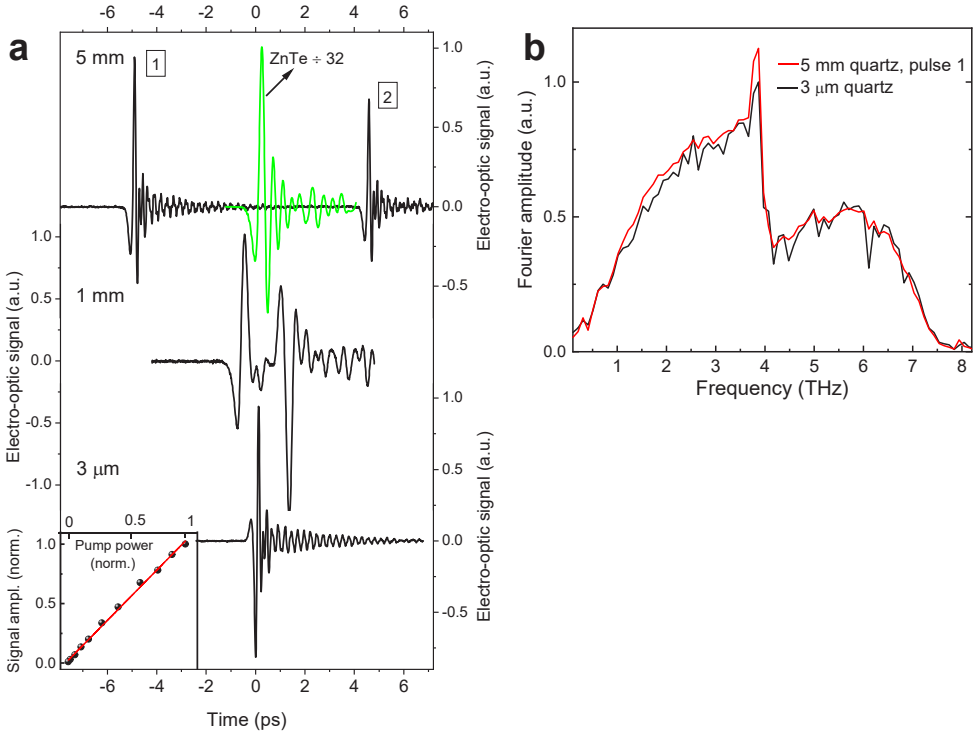

Fig. 2. Quartz THz emission. a) THz emission from quartz plates with 5 mm, 1 mm and 3 μm thicknesses. For the thick plates, two time-separated pulses can be distinguished. For the thinnest plate only one signal can be observed. Note that all signals have comparable amplitudes. For comparison the THz emission of a 500 μm thick ZnTe crystal measured in the same experimental setup as that of quartz is also given, the green signal. Note the ~32 scaling factor of the ZnTe signal. b) The Fourier spectrum of the first THz pulse of the 5 mm thick quartz and that of the 3 μm thick quartz are fully comparable. The sharp peak at ~4 THz corresponds to the oscillations in time-domain signals and matches the resonances of the phonon modes of the quartz.

Optics EXPRESS

fluence dependence of the observed THz signal from the thin quartz plate is given in the inset in the lowest panel of Fig. 2(a) and shows linear dependence of the emitted THz with 800 nm pump power.

We have also measured the azimuthal dependence of the THz emission from the quartz plates with thicknesses 5 mm and 3 μm. The polar plots of the resulting signals are shown in Fig. 3. All emitted signals show six maxima, the characteristic emission pattern of a system with three-fold symmetry. However, there is a phase shift between the signals from the two radiations observed from the thick plates. In case of the 5 mm and 1 mm thick quartz plates, the azimuthal dependence of the first pulse and the second pulse have close to ~10 degrees and ~ 3 degrees offset, respectively.

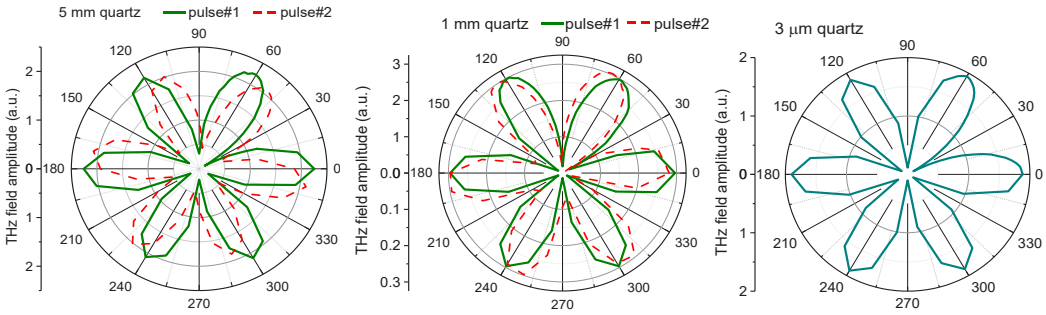

Fig. 3. Azimuthal dependence of quartz in THz emission. The azimuthal angle (φ) dependence of THz emission from quartz plates with thicknesses 5 mm, 1 mm and 3 μm are shown. While for the thin plate only one signal with six maxima as function of φ is resolved, for thick quartz plates the two delayed signals are phase shifted relative to each other.

2. Electro-optic sampling

In Fig. 4(a) we show the EOS response of quartz plates with different thicknesses, after pumping the crystals with intense LN THz pulses. For the thickest crystal (5 mm thick) two distinct responses separated by ~9.2 ps can clearly be resolved. In this experiment, the quartz plate is located such that the focus of the THz pulse is close to its center. Thereby, the probe pulse mixes with the spatially broad THz pulse on the two endings of the quartz plate. In addition, the THz pulse -generated via the pump pulse tilting technique in the lithium niobate crystal- suffers from large aberrations [52] thus, its waveform is resolved broader than the one measured with thinner crystals. For thinner crystals (1 mm and 0.5 mm) also the contribution of two signals can be realized. For thinner crystals <100 μm only a single signal, resembling the waveform of the THz electric field measured with 250 μm thick GaP is resolved, see the red line in the lowest panel of Fig. 4(a). To avoid saturation of the EOS in GaP, 8 silicon plates, each 200 μm thick are placed in the THz path. Also note that for the thin quartz plates, no reflective echo signals are observed. Due to the large THz wavelength, the internal reflections in ultra-thin plates are all within the main pulse of the THz.

Notably both in the THz emission and in the EOS signals of quartz, the delay of the two signals for different crystal thicknesses cannot be explained by the internal reflection of the THz pulses or the optical pump beam inside quartz. For instance, the echo signals of a THz pulse inside a 5 mm thick quartz should appear at ~66 ps after the first pulse, much longer than the observed ~9.3 ps delay of the observed signals in our experiment.

It is also important to express that there is a puzzling aspect of the EOS and THz emission signals of quartz, namely the amplitude of the latter signals is seemingly and to a good extent independent of the thickness of the quartz plates. In contrast, by increasing the effective thickness

Optics EXPRESS

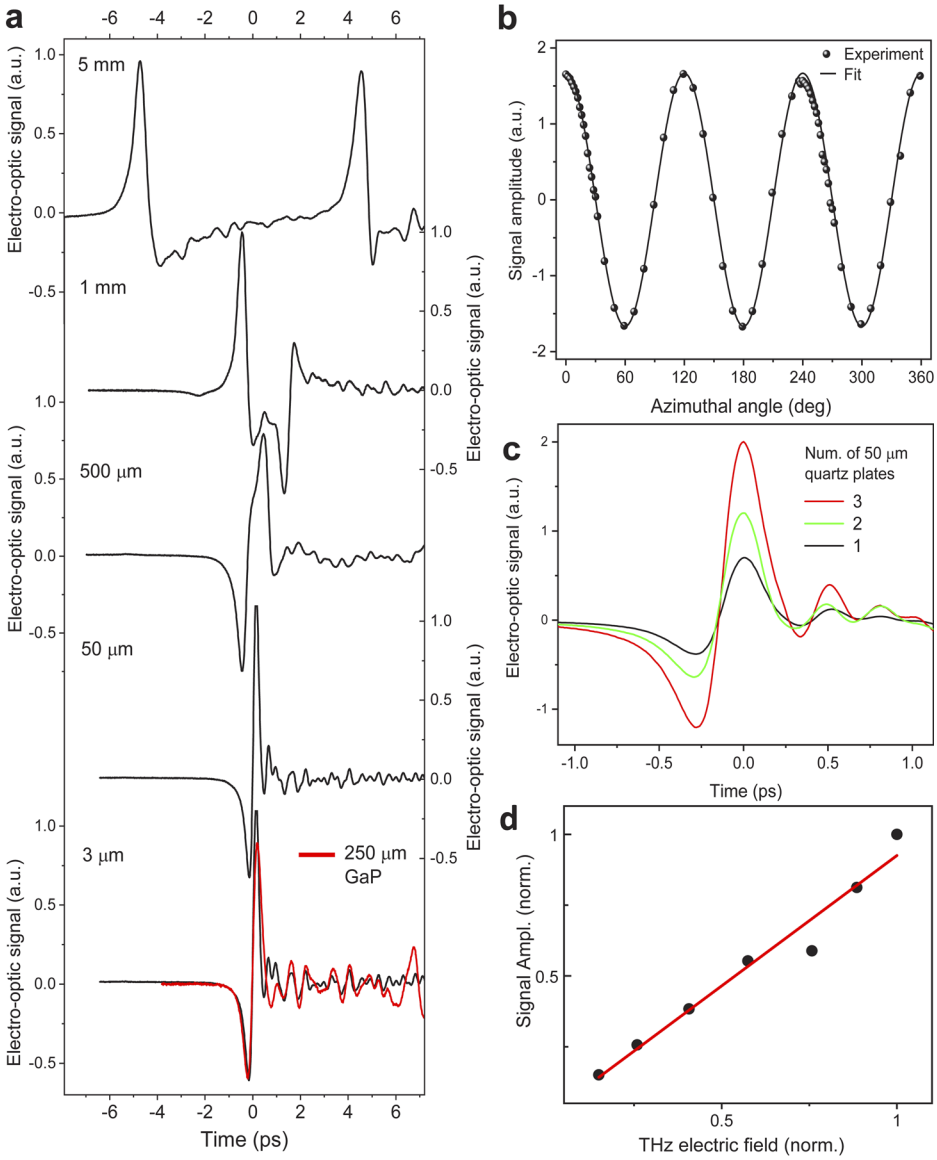

Fig. 4. THz detection with quartz plates. a) EOS signals of quartz plates with different thicknesses. Below the thickness of ~100 μm the shape and the amplitude of the signals stay unchanged. For 5 mm and 1 mm thick crystals two signals separated, respectively, by ~10 ps and ~ 2ps are observed. The time delays between the two pulses can be explained by the velocity mismatch between a THz pulse and a 800 nm pulse traversing the 5 mm and 1 mm quartz plates, respectively. For the intermediate thickness of 500 μm the two signals are merged. b) Azimuthal dependence of the EOS signal measured by the 50 μm thick quartz. c) While the EOS signal amplitudes of quartz plates in panel a are all comparable, the signal amplitude increases proportionally to the number quartz plates (each 50 μm thick) forming a stack. d) Fluence dependence of the EOS with 3 μm quartz plate scales linearly with THz electric field. The maximum electric field is 2 MV/cm. Note that the error bars are smaller than the data points.

Optics EXPRESS

of the crystals by stacking quartz plates, each 50 μm thick, the signal amplitude is accordingly increased. Here before stacking, each plate is aligned independently for its maximum EOS response with respect to its azimuthal angle. As displayed in Fig. 4(c), the amplitude of the signals increases proportional to the number of quartz plates. We have also performed the fluence dependence of the electro-optic sampling response of the 3 µm thick quartz. As shown in Fig. 4(d), the EOS signal of quartz scales linearly with the THz electric field strength, expected for a second-order nonlinear effect. The THz electric field strength is obtained via measuring the THz power with a calibrated power meter and converting it to the THz electric field strength via the proportionality of the power and the square of the THz electric field. The maximum THz field strength is obtained via the knife-edge technique [33].

We measured the azimuthal dependence of the EOS response of quartz, see Fig. 4(b). Similar to the azimuthal pattern of the quartz plates in the THz emission experiment, the resolved signals show six maxima. The solid line is a fit to the experimental data points using $\cos 3\varphi$ as the fitting equation, with φ serving as the azimuthal angle.

To obtain the spectral broadness of the EOS response of quartz, we have measured the EOS signal of a thin quartz plate after pumping the crystals with intense THz pulses of the STE. Figure 5(a) and 5(b) display the time-trace of the EOS response of quartz and the Fourier spectrum of the measured waveform, respectively. For comparison we have measured the same THz waveform using 10 μm thick ZnTe as the EO medium. Interestingly, the quartz response is extended almost up to 8 THz, with two sharp peaks appearing at 4 THz and 8 THz, the phonon modes of quartz [47]. The EOS response of thin quartz plates resembles its emission pattern, see Fig. 2(b).

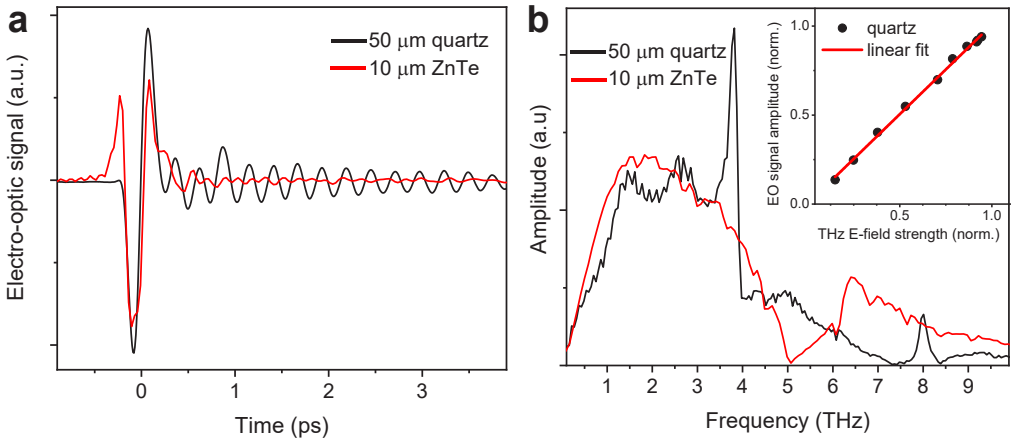

Fig. 5. Broadband THz detection. a) Time-domain EOS response of a quartz plate with 50 µm thickness pumped with the emission from a spintronic THz emitter (STE). The THz field strength is about 300KV/cm b) Fourier spectrum of the wave in panel a (black line) is compared to the STE emission measured with a 10 µm thick ZnTe crystal (red line). The inset shows the EOS signal measured with quartz, which scales linearly with the THz pump power.

3. Discussion

As mentioned above, the z-cut quartz has a broken centrosymmetry. The crystal has three-fold rotational symmetry along its c-axis and two-fold symmetry around a-axis. It belongs to the point group 32, Hermann-Mauguin notation [53]. For this symmetry group, crystals have two

Optics EXPRESS

nonzero tensor elements of the effective second-order susceptibility, for quartz these are d_{14}= 0.6 and d_{11}=1.41 [54].

The type II phase matching for OR and EOS processes in this symmetry group follows a second-order nonlinearity which depends on the internal phase-matching angle θ and azimuthal angle, this yields $d_{eff} = d_{11} \cos\theta\cos 3\varphi$ [55]. In our experiments, in which the THz wave and the optical beam co-propagate along the c-axis of the quartz plates, the internal angle $\theta = 0$, hence the effective second-order susceptibility is reduced to

$$d_{eff} = d_{11} \cos 3\varphi. \tag{1}$$

This implies that the amplitude of the EOS and OR signals of quartz would appear with six maxima with respect to azimuthal angle φ [56–59]. This agrees well with our experimental results presented in Fig. 3 and Fig. 4(b).

We also employ a simple analytical model to describe THz emission via OR and EOS signals of quartz. For simplicity we ignore reflections at the crystal surfaces and losses due to the absorption in optical and THz pulses, which are well justified for quartz at optical and THz frequencies. In both OR and EOS processes the phase matching condition in collinear geometry of difference frequency mixing is given by $\Delta K(\Omega, \omega) = K(\omega - \Omega) + K(\Omega) - K(\omega)$, where Ω and ω are, respectively the THz and the optical frequencies. The latter mismatch can be approximated as $\Delta K(\Omega, \omega) \approx \frac{\Omega}{c}[n(\Omega) - n_g(\omega)]$, where c is the speed of light, $n(\Omega)$ is the refractive index of the medium at THz frequency range, $n_g(\omega) = n(\omega) - \frac{\delta n(\omega)}{\delta\omega}$ is the group refractive index of the nonlinear medium at optical frequencies [59,60].

As the difference in the refractive indexes at optical THz frequencies of quartz is relatively large, the effective phase matching length, namely its coherence length, $l_c = \pi/\Delta K$, is short and decreases monotonically by increasing THz frequency from $l_c \approx 300$ μm @1 THz to $l_c \approx 50$ μm @5 THz.

For such system, as derived by Gallot and Grischkowsky, the phase factor in OR and EOS processes for a crystal with thickness d is given by [59,60]

$$P(\Omega) \propto i(1 - e^{-i\Delta K(\Omega,\omega)d}), \tag{2}$$

Using Eq. (1), the time profile of the THz pulse can be calculated via the inverse Fourier transform [54,61,62]

$$E_{\mathrm{THz}}(t) \propto \mathcal{F}^{-1}\left[\frac{\Omega^2 \cdot \mathrm{P}(\Omega) \cdot \mathrm{d} \cdot I(\Omega)}{\Delta K(\Omega, \omega)}\right], \tag{3}$$

in which $I(\Omega)$=$I_0(\Omega)e^{-\frac{\tau^2\Omega^2}{2}}$ is the Fourier spectrum of the optical pulse, assumed to have Gaussian temporal shape with bandwidth τ.

The detected THz electric field via EOS can also be calculated using the same phase factor in Eq. (2). Here the resolved signal can be obtained via [63–65]

$$S(t) \propto \mathcal{F}^{-1}\left[\frac{P(\Omega)E_{\mathrm{THz}}(\Omega)}{\Delta K(\Omega, \omega)}\right] \tag{4}$$

Using Eq. (3) and Eq. (4), we have calculated the emitted THz pulse and also the expected signal in the EOS process of quartz with different thicknesses. Interestingly, as shown in Fig. 6 the time-separated THz fields observed in thick quartz plates are captured in the calculated signals as well. It is worth mentioning that the two well separated THz emission signals have been observed previously for thick ZnTe, $LiNbO_3$ and $LiTaO_3$ crystals, too [66,67].

Note that the time delay between the observed signals in thick crystals, matches the time delay between a THz pulse and an optical pulse traversing the width of the crystals. With higher refractive index $n_{\mathrm{THz}} = 2.094$ @1.5 THz, the THz pulse lags behind the optical pulse with

Optics EXPRESS

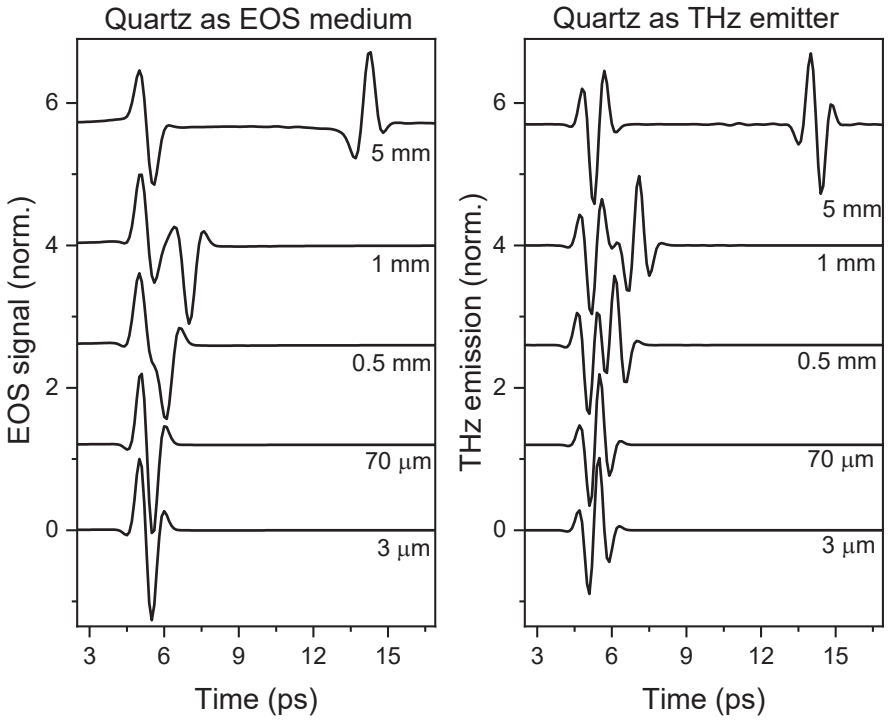

Fig. 6. Optical rectification and Electro-optic sampling in quartz, modeling. The left panel shows the modeled EOS signals of quartz for different thicknesses. The right panel shows the modeled THz emission from quartz as in left panel. For details see text. The modeled signals are shifted vertically for clarity.

refractive index n_{opt} =1.5383 @800 nm. For instance, the time delay between the two THz pulses generated at the two faces of 5 mm thick crystal will be ~9.2 ps using the relation $\Delta\tau = d\ c^{-1}\Delta n$, where $\Delta n = n_{THz} - n_{opt}$ is the difference between the refractive indexes of quartz at THz and optical frequencies. As illustrated by J. van der Valk et al. the dual signals in thick crystals can be explained by scrutinizing Eq. (2) [59]. The first term in Eq. (2) explains the THz generation and EOS on the front and rear sides of the crystal with the effective bulk contribution given by the coherent length of the OR and EOS processes in a crystal, with an additional phase shift due to the phase mismatch in the generation and detection processes.

Although the observation of the two separated THz pulses in one crystal can be explained by this simple model, the fairly constant amplitude of the OR and EOS signals and scaling of the THz field amplitude with the number of stacked layers (Fig. 4(c)) remains still puzzling. This is contrary to the expected signals from typical nonlinear media, in which the amplitude of the resolved signals scales with the thickness of the nonlinear medium. A plausible explanation can be the strong or even dominant contribution of quartz-air interface to the observed signals. Note that the contribution of bulk to the second-order nonlinear response is typically larger than that of the surface. However, as recently shown in a phase sensitive Sum Frequency Generation (SFG) spectroscopy experiment the quartz has a relatively large surface response, comparable with the contribution of its bulk to the SFG response [45]. As such, contribution from the surface may compensate the lower bulk contribution into the resolved signals.

Unfortunately, extracting the surface contribution to the OR and EOS turned out to be challenging. In an effort we modified the surface of the quartz by etching its surface to 10s of nanometer. However, we observed no difference between the EOS signals from etched and

Optics EXPRESS

non-etched quartz plates, most likely due to failing to turn the crystalline structure of quartz to an amorphous surface by etching.

In conclusion, we have characterized the THz emission and coherent THz detection of intense THz pulses in z-cut α-quartz plates. The emitted THz wave has a broad spectrum extended up to ~8 THz. The same spectral bandwidth is observed in the EOS response of thin α-quartz plates. Due to the small effective second-order nonlinearity of quartz the waveform of intense THz electric fields with strength as high as 2 MV/cm can be measured without saturation of the EOS process in α-quartz. Moreover, because of the large bandgap of quartz, the THz generation and detection can be realized using very wide frequency range of laser pulses from UV to IR. Strikingly, we found that the amplitude of OR and EOS signals are seemingly independent of the quartz thickness. This may strongly indicate a dominant contribution of the air-quartz interface on the THz response of quartz.

Funding. H2020 Marie Skłodowska-Curie Actions (MSCA-IF-2020-101030872).

Acknowledgements. Authors would like to thank Mathias Kläui and Gerhard Jakob for valuable discussions, comments on the manuscript and ion etching of a quartz plate.

Disclosures. The authors declare no conflicts of interest.

Data availability. The data that support the findings of this study are available from the corresponding author upon reasonable request.

References

1. M. Schirmer, M. Fujio, M. Minami, J. Miura, T. Araki, and T. Yasui, "Biomedical applications of a real-time terahertz color scanner," Biomed. Opt. Express **1**(2), 354 (2010).
2. M. C. Kemp, P. F. Taday, B. E. Cole, J. A. Cluff, A. J. Fitzgerald, and W. R. Tribe, "Security applications of terahertz technology," Terahertz Mil. Secur. Appl. **5070**(2003), 44 (2003).
3. A. Y. Pawar, D. D. Sonawane, K. B. Erande, and D. V. Derle, "Terahertz technology and its applications," Drug Invent. Today **5**(2), 157–163 (2013).
4. E. Pickwell and V. P. Wallace, "Biomedical applications of terahertz technology," J. Phys. D: Appl. Phys. **39**(17), R301–R310 (2006).
5. I. Mehdi, J. V. Siles, C. Lee, and E. Schlecht, "THz diode technology: Status, prospects, and applications," Proc. IEEE **105**(6), 990–1007 (2017).
6. N. Nagai, R. Kumazawa, and R. Fukasawa, "Direct evidence of inter-molecular vibrations by THz spectroscopy," Chem. Phys. Lett. **413**(4-6), 495–500 (2005).
7. M. Nagai, H. Yada, T. Arikawa, and K. Tanaka, "Terahertz time-domain attenuated total reflection spectroscopy in water and biological solution," Int. J. Infrared Millimeter Waves **27**(4), 505–515 (2006).
8. C. Rønne, P.-O. Åstrand, and S. Keiding, "THz Spectroscopy of Liquid H_2O and D_2O," Phys. Rev. Lett. **82**(14), 2888–2891 (1999).
9. M. Takahashi, "Terahertz vibrations and hydrogen-bonded networks in crystals," Crystals **4**(2), 74–103 (2014).
10. S. S. Zhukov, V. Balos, G. Hoffman, S. Alom, M. Belyanchikov, M. Nebioglu, S. Roh, A. Pronin, G. R. Bacanu, P. Abramov, M. Wolf, M. Dressel, M. H. Levitt, R. J. Whitby, B. Gorshunov, and M. Sajadi, "Rotational coherence of encapsulated ortho and para water in fullerene-C_{60} revealed by time-domain terahertz spectroscopy," Sci. Rep. **10**(1), 18329 (2020).
11. B. Sensale-Rodriguez, R. Yan, M. M. Kelly, T. Fang, K. Tahy, W. S. Hwang, D. Jena, L. Liu, and H. G. Xing, "Broadband graphene terahertz modulators enabled by intraband transitions," Nat. Commun. **3**(1), 780 (2012).
12. M. Karakus, S. A. Jensen, F. D'Angelo, D. Turchinovich, M. Bonn, and E. Cánovas, "Phonon-Electron Scattering Limits Free Charge Mobility in Methylammonium Lead Iodide Perovskites," J. Phys. Chem. Lett. **6**(24), 4991–4996 (2015).
13. R. Dong, P. Han, H. Arora, M. Ballabio, M. Karakus, Z. Zhang, C. Shekhar, P. Adler, P. S. Petkov, A. Erbe, S. C. B. Mannsfeld, C. Felser, T. Heine, M. Bonn, X. Feng, and E. Cánovas, "High-mobility band-like charge transport in a semiconducting two-dimensional metal–organic framework," Nat. Mater. **17**(11), 1027–1032 (2018).
14. Z. Mics, K. J. Tielrooij, K. Parvez, S. A. Jensen, I. Ivanov, X. Feng, K. Müllen, M. Bonn, and D. Turchinovich, "Thermodynamic picture of ultrafast charge transport in graphene," Nat. Commun. **6**(1), 7655 (2015).
15. L. Ozyuzer, A. E. Koshelev, C. Kurter, N. Gopalsami, Q. Li, M. Tachiki, K. Kadowaki, T. Yamamoto, H. Minami, H. Yamaguchi, T. Tachiki, K. E. Gray, W. K. Kwok, and U. Welp, "Emission of coherent THz radiation from superconductors," Science **318**(5854), 1291–1293 (2007).
16. M. Beck, M. Klammer, S. Lang, P. Leiderer, V. V. Kabanov, G. N. Gol'tsman, and J. Demsar, "Energy-gap dynamics of superconducting NbN thin films studied by time-resolved terahertz spectroscopy," Phys. Rev. Lett. **107**(17), 177007 (2011).

Optics EXPRESS

17. V. Balos, S. Imoto, R. R. Netz, M. Bonn, D. J. Bonthuis, Y. Nagata, and J. Hunger, "Macroscopic conductivity of aqueous electrolyte solutions scales with ultrafast microscopic ion motions," Nat. Commun. **11**(1), 1611 (2020).
18. G. Schwaab, F. Sebastiani, and M. Havenith, "Ion Hydration and Ion Pairing as Probed by THz Spectroscopy," Angew. Chem. Int. Ed. **58**(10), 3000–3013 (2019).
19. A. G. Markelz, A. Roitberg, and E. J. Heilweil, "Pulsed terahertz spectroscopy of DNA, bovine serum albumin and collagen between 0.1 and 2.0 THz," Chem. Phys. Lett. **320**(1-2), 42–48 (2000).
20. S. J. Kim, B. Born, M. Havenith, and M. Gruebele, "Real-time detection of protein-water dynamics upon protein folding by terahertz absorption spectroscopy," Angew. Chem. Int. Ed. **47**(34), 6486–6489 (2008).
21. V. Balos, M. Bonn, and J. Hunger, "Quantifying transient interactions between amide groups and the guanidinium cation," Phys. Chem. Chem. Phys. **17**(43), 28539–28543 (2015).
22. V. Balos, M. Bonn, and J. Hunger, "Correction: Quantifying transient interactions between amide groups and the guanidinium cation," Phys. Chem. Chem. Phys. **18**(2), 1346–1347 (2016).
23. V. Balos, H. Kim, M. Bonn, and J. Hunger, "Dissecting Hofmeister Effects: Direct Anion-Amide Interactions Are Weaker than Cation-Amide Binding," Angew. Chemie - Int. Ed. **55**(28), 8125–8128 (2016).
24. V. Balos, B. Marekha, C. Malm, M. Wagner, Y. Nagata, M. Bonn, and J. Hunger, "Specific Ion Effects on an Oligopeptide: Bidentate Binding Matters for the Guanidinium Cation," Angew. Chem. Int. Ed. **58**(1), 332–337 (2019).
25. A. Shalit, S. Ahmed, J. Savolainen, and P. Hamm, "Terahertz echoes reveal the inhomogeneity of aqueous salt solutions," Nat. Chem. **9**(3), 273–278 (2017).
26. H. Elgabarty, T. Kampfrath, D. J. Bonthuis, V. Balos, N. K. Kaliannan, P. Loche, R. R. Netz, M. Wolf, T. D. Kühne, and M. Sajadi, "Energy transfer within the hydrogen bonding network of water following resonant terahertz excitation," Sci. Adv. **6**(17), 1–9 (2020).
27. M. Sajadi, M. Wolf, and T. Kampfrath, "Transient birefringence of liquids induced by terahertz electric-field torque on permanent molecular dipoles," Nat. Commun. **8**(1), 14963 (2017).
28. V. Balos, N. K. Kaliannan, H. Elgabarty, M. Wolf, T. D. Kühne, and M. Sajadi, "Time-resolved terahertz-Raman spectroscopy reveals that catios and anions distinctly modify intermolecular interactions of water," Nat. Chem. **14**(9), 1031–1037 (2022).
29. S. F. Maehrlein, P. P. Joshi, L. Huber, F. Wang, M. Cherasse, Y. Liu, D. M. Juraschek, E. Mosconi, D. Meggiolaro, F. De Angelis, and X. Y. Zhu, "Decoding ultrafast polarization responses in lead halide perovskites by the two-dimensional optical Kerr effect," Proc. Natl. Acad. Sci. U.S.A. **118**(7), 1–7 (2021).
30. H. A. Hafez, S. Kovalev, J. C. Deinert, Z. Mics, B. Green, N. Awari, M. Chen, S. Germanskiy, U. Lehnert, J. Teichert, Z. Wang, K. J. Tielrooij, Z. Liu, Z. Chen, A. Narita, K. Müllen, M. Bonn, M. Gensch, and D. Turchinovich, "Extremely efficient terahertz high-harmonic generation in graphene by hot Dirac fermions," Nature **561**(7724), 507–511 (2018).
31. V. Balos, G. Bierhance, M. Wolf, and M. Sajadi, "Terahertz-Magnetic-Field Induced Ultrafast Faraday Rotation of Molecular Liquids," Phys. Rev. Lett. **124**(9), 093201 (2020).
32. P. Salén, M. Basini, S. Bonetti, J. Hebling, M. Krasilnikov, A. Y. Nikitin, G. Shamuilov, Z. Tibai, V. Zhaunerchyk, and V. Goryashko, "Matter manipulation with extreme terahertz light: Progress in the enabling THz technology," Phys. Rep. **836-837**, 1–74 (2019).
33. M. Sajadi, M. Wolf, and T. Kampfrath, "Terahertz-field-induced optical birefringence in common window and substrate materials," Opt. Express **23**(22), 28985–28992 (2015).
34. T. Seifert, S. Jaiswal, M. Sajadi, G. Jakob, S. Winnerl, M. Wolf, M. Kläui, and T. Kampfrath, "Ultrabroadband single-cycle terahertz pulses with peak fields of 300 kV cm^{-1} from a metallic spintronic emitter," Appl. Phys. Lett. **110**(25), 252402 (2017).
35. T. Seifert, S. Jaiswal, and U. Martens, *et al.*, "Efficient metallic spintronic emitters of ultrabroadband terahertz radiation," Nat. Photonics **10**(7), 483–488 (2016).
36. Y. S. Lee, T. Meade, V. Perlin, H. Winful, T. B. Norris, and A. Galvanauskas, "Generation of narrow-band terahertz radiation via optical rectification of femtosecond pulses in periodically poled lithium niobate," Appl. Phys. Lett. **76**(18), 2505–2507 (2000).
37. F. D'Angelo, Z. Mics, M. Bonn, and D. Turchinovich, "Ultra-broadband THz time-domain spectroscopy of common polymers using THz air photonics," Opt. Express **22**(10), 12475 (2014).
38. Q. Wu and X. C. Zhang, "Free-space electro-optic sampling of terahertz beams," Appl. Phys. Lett. **67**(24), 3523–3525 (1995).
39. A. Nahata, D. H. Auston, T. F. Heinz, and C. Wu, "Coherent detection of freely propagating terahertz radiation by electro-optic sampling," Appl. Phys. Lett. **68**(2), 150–152 (1996).
40. A. Nahata, A. S. Weling, and T. F. Heinz, "A wideband coherent terahertz spectroscopy system using optical rectification and electro-optic sampling," Appl. Phys. Lett. **69**(16), 2321–2323 (1996).
41. H. Hirori, A. Doi, F. Blanchard, and K. Tanaka, "Single-cycle terahertz pulses with amplitudes exceeding 1 MV/cm generated by optical rectification in $LiNbO_3$," Appl. Phys. Lett. **98**(9), 091106–5 (2011).
42. V. G. Dmitriev, G. G. Gurzadyan, and D. N. Nikogosyan, Handbook of Nonlinear Optical Crystals (Springer, 1999).
43. C. Bosshard, K. Sutter, P. Pretre, J. Hulliger, M. Flörsheimer, P. Kaatz, and P. Günter, "Organic Nonlinear Optical Materials," in *Advances in Nonlinear Optics*, Gordon and Breach, ed. (1995).

Optics EXPRESS

44. F. Zernike and P. R. Berman, "Generation of far infrared as a difference frequency," Phys. Rev. Lett. **15**(26), 999–1001 (1965).
45. M. Thämer, T. Garling, R. K. Campen, and M. Wolf, "Quantitative determination of the nonlinear bulk and surface response from alpha-quartz using phase sensitive SFG spectroscopy," J. Chem. Phys. **151**(6), 064707 (2019).
46. Q. Wu, M. Litz, and X. C. Zhang, "Broadband detection capability of ZnTe electro-optic field detectors," Appl. Phys. Lett. **68**(21), 2924–2926 (1996).
47. C. L. Davies, J. B. Patel, C. Q. Xia, L. M. Herz, and M. B. Johnston, "Temperature-Dependent Refractive Index of Quartz at Terahertz Frequencies," J. Infrared, Millimeter, Terahertz Waves **39**(12), 1236–1248 (2018).
48. L. Zhu, Y. Huang, Z. Yao, B. Quan, L. Zhang, J. Li, C. Gu, X. Xu, and Z. Ren, "Enhanced polarization-sensitive terahertz emission from vertically grown graphene by a dynamical photon drag effect," Nanoscale **9**(29), 10301–10311 (2017).
49. Z. Fan, M. Xu, Y. Huang, Z. Lei, L. Zheng, Z. Zhang, W. Zhao, Y. Zhou, X. Wang, X. Xu, and Z. Liu, "Terahertz Surface Emission from $MoSe_2$at the Monolayer Limit," ACS Appl. Mater. Interfaces **12**(42), 48161–48169 (2020).
50. J. Hebling, K.-L. Yeh, M. C. Hoffmann, B. Bartal, and K. A. Nelson, "Generation of high-power terahertz pulses by tilted-pulse-front excitation and their application possibilities," J. Opt. Soc. Am. B **25**(7), B6 (2008).
51. V. Balos, P. Müller, G. Jakob, M. Kläui, and M. Sajadi, "Imprinting the complex dielectric permittivity of liquids into the spintronic terahertz emission," Appl. Phys. Lett. **119**(9), 091104 (2021).
52. C. Vicario, B. Monoszlai, and C. P. Hauri, "GV/ m single-cycle terahertz fields from a laser-driven large-size partitioned organic crystal," Phys. Rev. Lett. **112**(21), 213901 (2014).
53. G. L. Breneman, "Crystallographic symmetry point group notation flow chart," J. Chem. Educ. **64**(3), 216–217 (1987).
54. T. S. Narasimhamurty, *Photoelastic and ElectroßOptic Properties of Crystals* (Plenum Press, 1981).
55. J. E. Midwinter and J. Warner, "The effects of phase matching method and of uniaxial crystal symmetry on the polar distribution of second-order non-linear optical polarization," Br. J. Appl. Phys. **16**(8), 1135–1142 (1965).
56. Y. Huang, Z. Yao, C. He, L. Zhu, L. Zhang, J. Bai, and X. Xu, "Terahertz surface and interface emission spectroscopy for advanced materials," J. Phys.: Condens. Matter **31**(15), 153001 (2019).
57. P. C. M. Planken, H.-K. Nienhuys, H. J. Bakker, and T. Wenckebach, "Measurement and calculation of the orientation dependence of terahertz pulse detection in ZnTe," J. Opt. Soc. Am. B **18**(3), 313 (2001).
58. A. Rice, Y. Jin, X. F. Ma, X. C. Zhang, D. Bliss, J. Larkin, and M. Alexander, "Terahertz optical rectification from ‹110› zinc-blende crystals," Appl. Phys. Lett. **64**(11), 1324–1326 (1994).
59. N. C. J. van der Valk, P. C. M. Planken, A. N. Buijserd, and H. J. Bakker, "Influence of pump wavelength and crystal length on the phase matching of optical rectification," J. Opt. Soc. Am. B **22**(8), 1714 (2005).
60. Y. R. Shen, "Far-infrared generation by optical mixing," Prog. Quantum Electron. **4**(PART 3), 207–232 (1976).
61. A. Schneider, M. Neis, M. Stillhart, B. Ruiz, R. U. A. Khan, and P. Günter, "Generation of terahertz pulses through optical rectification in organic DAST crystals: theory and experiment," J. Opt. Soc. Am. B **23**(9), 1822 (2006).
62. Z. Wang, "Generation of terahertz radiation via nonlinear optical methods," IEEE Trans. Geosci. Remote Sens. **1**(1), 1–5 (2002).
63. G. Gallot and D. Grischkowsky, "Electro-optic detection of terahertz radiation," J. Opt. Soc. Am. B **16**(8), 1204 (1999).
64. G. Gallot, J. Zhang, R. W. McGowan, T. I. Jeon, and D. Grischkowsky, "Measurements of the THz absorption and dispersion of ZnTe and their relevance to the electro-optic detection of THz radiation," Appl. Phys. Lett. **74**(23), 3450–3452 (1999).
65. A. Leitenstorfer, S. Hunsche, J. Shah, M. C. Nuss, and W. H. Knox, "Detectors and sources for ultrabroadband electro-optic sampling: Experiment and theory," Appl. Phys. Lett. **74**(11), 1516–1518 (1999).
66. L. Xu, X. C. Zhang, and D. H. Auston, "Terahertz beam generation by femtosecond optical pulses in electro-optic materials," Appl. Phys. Lett. **61**(15), 1784–1786 (1992).
67. T. Kampfrath, J. Nötzold, and M. Wolf, "Sampling of broadband terahertz pulses with thick electro-optic crystals," Appl. Phys. Lett. **90**(23), 231113–4 (2007).